pH-Dependent Behavior of Hydrophobically Modified Polyelectrolyte Shells of Polymeric Nanoparticles

Karel Procházka,[*1] *Pavel Matějíček,*[1] *Mariusz Uchman,*[1] *Miroslav Štěpánek,*[1] *Jana Humpolíčková,*[2] *Martin Hof,*[2] *Milena Špírková*[3]

Summary: The self-assembled core-shell nanoparticles based on fluorescently double-tagged high-molar-mass polystyrene-*block*-poly(methacrylic acid), PS-PMA, were prepared in aqueous buffers by dialysis from 1,4-dioxane – water mixtures. The conformations of shell-forming PMA chains were studied using nonradiative excitation energy transfer measurements. The study shows that two populations of distinctly different conformations (collapsed and stretched) coexist in the shell and their ratio depends on pH.

Keywords: block polyelectrolyte micelles; light scattering; nonradiative excitation energy transfer; time-resolved fluorescence

Introduction

Amphiphilic block copolymers containing a long hydrophobic (HP) block, such as polystyrene, PS, and a long weak polyelectrolyte (PE) block, such as poly(methacrylic acid), PMA are insoluble in aqueous media, because water is nonsovent for HP block. However, the self-assembled core-shell nanoparticles, containing HP core and water-soluble shell can be prepared indirectly, e.g., by dialysis.[1] The PS-PMA copolymers dissolve in moderately polar organic solvents (e.g., in 1,4-dioxane). A consequent stepwise dialysis against mixtures with increasing content of water yields the self-assembled core-shell nanoparticles. During dialysis, the thermodynamic quality of the mixed solvent deteriorates sharply for PS, but remains almost constant for PMA, because water is marginal solvent (slightly below θ-state) for neutral (non-dissociated) PMA.[2] The association number, density and viscosity of PS cores grow with increasing water content, while the concentration of free chains (unimers) decreases. At a certain ''critical composition'', the solvent quality is so bad for PS that the cores become glassy (the glass transition temperature of PS nanodomains, T_G, is lower than that of bulk PS, but is still well above ambient temperature[3]). Simultaneously, the concentration of unimers drops to zero and the exchange of unimers between micelles stops (the micellization equilibrium kinetically freezes). With further increase in water content, the association number does not change any more. In water-rich alkaline solvents, the dissociation of carboxylic groups occurs and solvent quality for PMA improves. The kinetically frozen core-shell micelle can be regarded as an inert PS sphere decorated by the PMA brush which is tethered to its surface. Aqueous solutions of PS-PMA micelles are fairly stable in a broad pH range and their properties reflect the polyelectrolyte behavior of PMA shells.

A number of aqueous systems of micellizing polymers have been studied during last two decades[4–9] because they offer promising applications, e.g., as vehicles in

[1] Department of Physical and Macromolecular Chemistry, Charles University in Prague, Faculty of Science, Albertov 6, CZ-128 43 Praha 2, Czech Republic
[2] The Jaroslav Heyrovsky Institute of Physical Chemistry, Czech Academy of Sciences, Dolejškova 3, CZ-182 23 Prague 8, Czech Republic
[3] Institute of Macromolecular Chemistry, Czech Academy of Sciences, Heyrovsky Square 2, CZ-162 06, Prague 6 – Petřiny, Czech Republic

the targeted delivery of drugs.[10,11] We have been studying the self-assembly and behavior of kinetically frozen polymer nanoparticles in aqueous media by a combination of several experimental techniques (mainly by light scattering and fluorescence)[12–16] and by computer simulations[17] since early nineties of the last century. Several years ago, we started a systematic research of modified systems because the application of polymer micelles often requires their chemical modification (e.g., the attachment of targeting groups) and the modified systems behave differently from the parent ones.[18–20] In this communication, we present new results of fluorescence studies with the aim (i) to show how a relatively small modification can alter the conformational behavior of shell-forming chains, and (ii) to advertise enormous potential of fluorescence techniques for polymer self-assembly studies. When comparing new and the already published data, we guard a privilege to interpret them from the up-to date point of view.

Experimental Part

Block Copolymer Samples

The samples were prepared by anionic polymerization in the framework of our cooperation with the group of Prof. S. E. Webber at the University of Texas at Austin. The preparation and characterization was described in earlier papers.[21] The molar mass, M_w, PS weight fraction, w_{PS} and polydispersity index, M_w/M_n, of (i) single tagged, PS-N-PMA and (ii) double tagged sample, PS-N-PMA-A are the following: (i) 54.4 kg/mol, 0.42, 1.15 and (ii) 60.6 kg/mol, 0.52, 1.09, respectively.

Preparation and Characterization of Micelles

The micelles were prepared by stepwise dialysis from 1,4-dioxane – water mixtures (rich in 1,4-dioxane) to solvents with increasing water content and then transferred in buffers differing in pH as described in ref.[1] The final polymer concentration was evaluated according to volume changes during dialysis.

Light Scattering Measurements

The experimental setup (ALV, Langen, Germany) consisted of a He-Ne laser, operating at the wavelength $\lambda = 632.8$ nm, an ALV CGS/8F goniometer, an ALV High QE APD detector and an ALV 5000/EPP multibit, multitau autocorrelator. The solutions for measurements were filtered through 0.45 μm Acrodisc filters. The measurements were carried out for concentrations 0.4–1.8 g/L and different angles, θ, at 20 °C.

The dynamic light scattering (DLS) data were fitted using the constrained regularization algorithm (CONTIN) which provides the distribution of relaxation times τ, $A(\tau)$, as the inverse Laplace transform of $g^{(1)}(t)$ function, which can be obtained from the measured normalized autocorrelation function of the scattered light intensity $g^{(2)}(t)$ by the equation $g^{(2)}(t) = 1+\beta|g^{(2)}(t)|^2$. The apparent diffusion coefficient, D^{app}, (in case of diffusive motion) and the hydrodynamic radius, R_H were obtained by applying standard formulas as described elsewhere.[15,16]

Static light scattering (SLS) data were treated by the Zimm method as described elsewhere[15,16] Refractive index increments of tagged PS-PMA copolymers in aqueous media were measured with the Brice-Phoenix differential refractometer under osmotic equilibrium of low-molar-mass components in our earlier studies.[15,16]

Fluoromery

Steady-state fluorescence spectra were measured in 1 cm quartz cuvettes using a SPEX Fluorolog 3–11 fluorometer. Fluorescence decays were measured by the time-correlated single photon counting technique on an Edinburgh Instruments ED 299 T fluorometer equipped with a hydrogen-filled nanosecond coaxial discharge flash lamp (half-width of the pulse ca. 1.2 ns). The measured decays were fitted to the convolution of the multi-exponential function with the instrument response profile

using the Marquardt–Levenberg nonlinear least squares method as described elsewhere.[21]

Fluorescence Correlation Spectroscopy.

All measurements were performed with binocular microscope Confocor I, Carl Zeiss, Jena, Germany, equipped with a 514 nm argon laser, an adjustable pinhole together with a special fluorescence optics, detection diode SPCM-200PQ and a ALV-5000 correlator (ALV Langen, Germany) as described elsewhere[22]. The analysis of temporary fluctuations of fluorescence intensity assumes only the translational diffusion of micelles and photobleaching due to the intersystem crossing. The micelles were labeled with octadecylrhodamine B which is very little soluble in aqueous media (in the form of self-quenched non-fluorescent associates) and binds strongly to micelles in form of separated fluorescent molecules. Therefore only the fluorescence from labeled micelles contributes to the measured signal. Because the emission of octadecylrhodamine B is read-shifted with respect to both Np and An, their presence does not affect the measurement.

Atomic Force Microscopy (AFM)

The measurements were performed in the tapping mode under ambient conditions using a commercial scanning probe microscope, Digital Instruments NanoScope dimensions 3, equipped with a Nanosensors silicon cantilever, typical spring constant 40 N m^{-1}. Polymeric micelles were deposited on a fresh (i.e., freshly peeled out) mica surface (flogopite) by a fast dip coating in a dilute PS-PMA solution (c ca. 10^{-2} g/L). After the evaporation of water, the samples were dried in vacuum oven at ambient temperature for ca. 5 hours.

Nonradiative Exitation Energy Transfer in Double Tagged Micelles and Strategy of Fluorescence Study

Fluorescence techniques have become very popular in polymer research during last few decades, particularly after the wide-spread of commercially produced time-resolved fluorometers. Because the absorption and emission of a photon are separated by the time window of units to hundreds of ns, the emission is affected by processes that occur in the immediate vicinity of the fluorophore during the lifetime of the excited state. Therefore the fluorescence reports on interactions of the fluorophore with its nanoenvironment and on the dynamics of fast processes that proceed in its immediate vicinity. However, the fluorometry is an indirect technique and requires independent information for unambiguous interpretation of obtained results.

The nonradiative excitation energy transfer (NRET) is a suitable method for the investigation of the effect of pH on the conformational behavior of shell-forming PMA chains modified at the free end by a fairly large and strongly hydrophobic fluorescent group. We measured the time-resolved fluorescence decays of PS-PMA micelles tagged by one pendant naphthalene (Np) between blocks and one anthracene (An) the end of the PMA block. In micelles, all Np are embedded in a relatively rigid and nonpolar core-shell interface. A strongly hydrobhobic An attached at the end of PMA block tries to avoid the aqueous medium and buries in the shell which is less polar than water. A close An approach to the core requires that the PMA chain either collapses or recoils back forming an open loop. Both conformations lower entropy of the system. The ensemble average radial distribution of probes in the shell is a result of an intricate enthalpy-to-entropy interplay. The enthalpy part (differentiating the tagged from its parent PS-PMA system) comprises mainly the interaction of anthracene with the nanoenvironment and the entropy part reflects the difference in the number of possible conformations of tagged and parent shell-forming chains.

Besides the study of double-tagged PS-PMA micelles, we investigated a single tagged (Np) system to get the Np fluorescence decay from micelles unaffected by

NRET. The single tagged and double tagged samples are very similar, but they were synthesized independently and PS and PMA block lengths in both systems slightly differ.

Results and Discussion

The weight-average molar mass, M_w, (obtained from the Zimm plot by extrapolation to zero concentration and zero scattering angle) and the apparent hydrodynamic radius, R_H, (measured at low, albeit finite concentration and scattering angle 90^0) in 0.15 M borax are the following: (i) single tagged sample, $M_w = 8.00 \times 10^3$ kg/mol, $R_H = 40$ nm (ii) double-tagged sample, $M_w = 7.52 \times 10^3$ kg/mol, $R_H = 45$ nm. Angular DLS measurement proved that the scattering mode corresponds to the diffusion of individual nanoparticles (micelles) in both cases. Figure 1 shows the sigmoidal dependence of R_H on pH in buffers with a fairly low constant ionic strength, $I = 0.15$ mol/L for a double tagged sample. Insert in Figure 1 depicts the influence of I on R_H at constant pH 10.5. Both curves agree with results of our earlier studies on similar non-modified systems.[23] The number average molar mass of double tagged micelles, M_n, obtained by "SCF titration" as described in ref.[22], was the following $M_n = 5.47 \times 10^3$ kg/mol. The comparison of SLS and SCF data indicates reasonably low polydispersity of micelles prepared by dialysis.

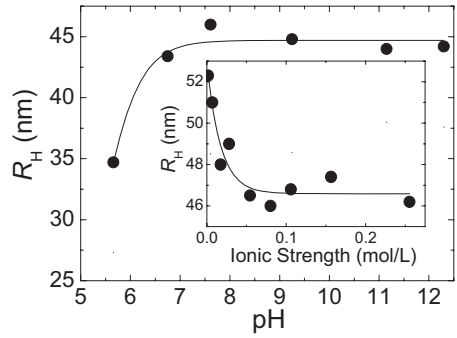

Figure 1.
Hydrodynamic radius, R_H, as a function of pH (ionic strength, $I = 0.15$ mol/L). **Inset**. Hydrodynamic radius, R_H, as a function of I (pH 10.5).

Spherical shapes and fairly low polydispersity of micelles can be documented by AFM scans of micelles deposited on a fresh mica surface (see Figure 2).

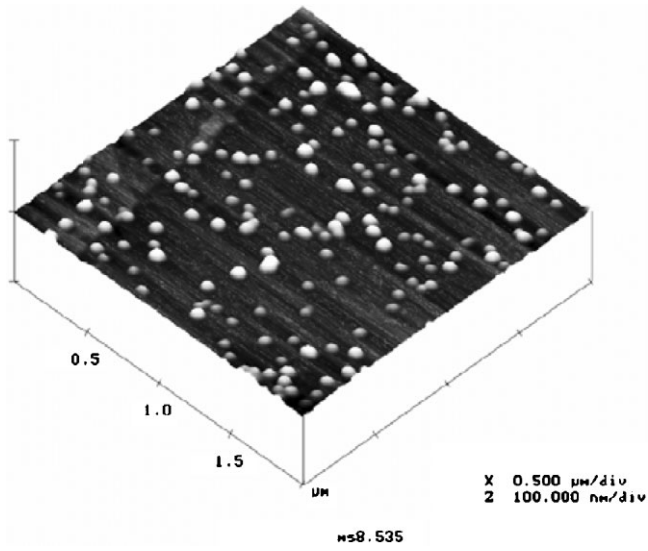

Figure 2.
AFM scan of hydrophobically modified PS-PMA micelles deposited on mica surface.

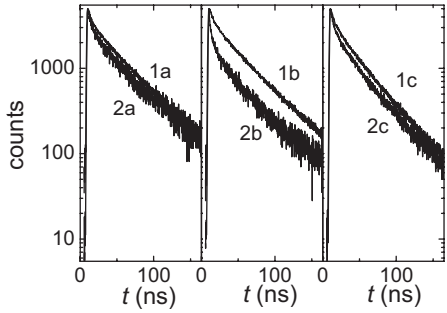

Figure 3.
Time resolved fluorescence decays of naphthalene fluorescence from the single tagged micelles (curves 1) and the double tagged micelles (curves 2) for pH = 4.3 (curves a), pH = 5.5 (curves b) and pH = 10.4 (curves c).

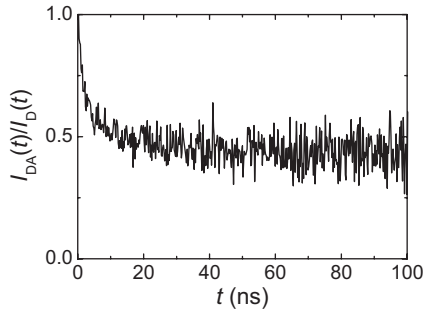

Figure 4.
The normalized time-resolved NRET quenching curve, $I_{DA}(t)/I_D(t)$, at pH = 5.5.

The micelles are pancake-deformed after their deposition and drying, because the PMA chains spread at the hydrophilic mica surface. The section analysis for a typical micelle (not shown) yields average vertical dimensions corresponding to the size of PS core, ca.10 nm. Average horizontal diameter corresponds to the size of a typical micelle with stretched PMA chain, ca. 90 nm.

The time-resolved fluorescence decays, $I_D(t)$ of naphthalene (donor) fluorescence from single-tagged micelles (curves 1), i.e., data that are non-affected by NRET, and decays from double-tagged micelles (curves 2), i.e. decays, $I_{DA}(t)$, that could be potentially affected by NRET to anthracene (acceptor), if the Np – An distances were comparable with the Förster radius, R_0 (2.1 nm in toluene[18]), are shown in Figure 3 for three pH 4.5 (a), 5.5 (b) and 10.4 (c). Despite the fact that the shell thickness is always 10–20 times larger than the Förster radius for the Np – An pair, the quenching of Np fluorescence by NRET is clearly obvious.

The normalized quenching effect, i.e., the ratio of the NRET-affected decay divided by the pertinent unaffected decay, $I_{DA}(t)/I_D(t)$, is shown in Figure 4. The plot reminds a ''broken-like'' curve consisting of two distinct parts: (i) steep initial decrease at early times upon excitation indicating a strong quenching of a fraction of excited Np donors and (ii) almost constant part of the curve at long times suggesting that many excited Np in the irradiated solution of micelles are not at all affected by NRET. In our earlier papers, we have shown that such type of ''broken'' decay curve is compatible only with a bimodal distribution of An distances from the core-shell interface.[18]

The NRET quenching in micellar systems with bimodal distribution of acceptors can be explained with the aid of Scheme 1. It depicts the conformations of shell forming chains in (i) parent non-modified system (upper left part), (ii) 100% modified system (right part) and (iii) partially modified system (lower left part). Let's focus on the 100% modified system only: Due to bimodal distribution of An distances, only

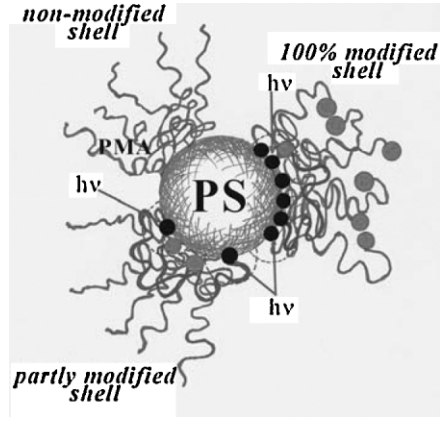

Scheme 1.
Conformations of modified and unmodified PMA chains in shells of PS-PMA micelles.

some Np have An neighbors in their immediate vicinity (closer than R_0). In current fluorescence measurements, only a low fraction of probes (ca. 10^{-6}) are excited. It corresponds to one probe *per* 10^4 micelles and a simultaneous excitation of several probes in one micelles can be neglected. If a Np with a close An neighbor is excited, the fluorescence is strongly quenched. However, an important fraction of potentially excited An do not have close An neighbors and, if excited, they exhibit the non-quenched fluorescence. The fraction of NRET-affected micelles corresponds to the fraction of An localized close to the core and, in the first approximation, is given by the total decrease in $I_{DA}(t)/I_D(t)$, i.e., by the value of the constant part of the normalized curve at long times.

The above outlined quenching mechanism was supported by results of our lattice Monte Carlo simulation of self-avoiding PMA chains tethered to the core surface.[24] In the simulation, the short range interactions were taken into account in calculating the Rosenbtuth weights and the long-range Coulomb forces were treated indirectly by solving the radial Poisson-Boltzmann (PB) equation. The energy of both contributions was used in the Metropolis criterion, which assured the self-consistency of the method. The simulations confirmed the bimodal distribution of An in the shell in a broad pH region. It also showed that chains with An located close to the core collapse but do not form open loops.

In the next part, we present new experimental data on changes in An distribution with pH and compare them with existing MC data which predict that increasing pH promotes the ionization and stretching of PMA chains, lowers the fraction of core-adsorbed hydrophobic acceptors (anthracene) and weakens the quenching effect. The experimental NRET efficiency, χ_{ET}, is depicted in Figure 5 as a function of pH. The curve has a pronounced non-monotonous shape with a maximum close to pH 5. The difference from the MC prediction is due to the fact the model used in MC simulation does not capture all

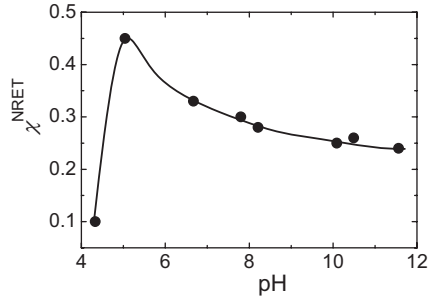

Figure 5.
The NRET efficiency, χ^{NRET}, as a function of pH.

details of the unique behavior in which PMA differs from the majority of weak PEs in poor solvents[25–27] and therefore the simulations describe general behavior of typical weak PE shells. It is a recognized fact, that the presence of methyl group in PMA does not only lowers the PMA solubility in aqueous media, but it also modifies substantially its properties as compared with other PEs, e.g., with PAA The conformational transition (i) is very pronounced, (ii) shifted towards fairly high pH, (iii) occurs in a very narrow pH region and (iv) the apparent dissociation constant, K_A^{app}, of PMA depends very strongly on the degree of ionization, α..

We have shown earlier that PMA shell consists of two regions differing in density, polarity and degree of dissociation: (i) dense ''hydrophobic'' layer containing collapsed parts of non-dissociated PMA chains close to the core and (ii) dilute part with fairly stretched and ionized chain ends close to the shell periphery.[28] They are separated by a narrow layer where all properties change very steeply. The sigmoidal (almost step-like) density profile of the PMA shell was confirmed also by small-angle neutron scattering (SANS) measurements by other authors.[29,30] An increase in pH promotes the overall ionization and reduces the density and width of the inner hydrophobic layer, nevertheless our studies with polarity-sensitive fluorophores indicated that even at fairly high pH, a thin ''hydrophobic'' layer persists close to the core.[12]

Based on previous arguments, the non-monotonous shape of experimental χ_{ET}, *vs.*

pH curve can be explained as follows: At low pH, the inner ''hydrophobic'' layer of non-dissociated PMA is quite thick and dense. A considerable fraction of An (attached to PMA) returns back towards the core, but due to fairly high density and sufficiently low polarity of the inner non-dissociated PMA layer, many An acceptors remain embedded relatively far from Np donors. Hence χ_{ET} is low despite the fact that the fraction of core-approaching An is high. Close to pK_A, the ionization starts to grow fast and both the thickness and density of the inner PMA decrease. In this pH region, a fairly high fraction of An still returns back towards the core. Two opposite effects compete and affect χ_{ET}: (i) The fraction of collapsing PMA chains (bearing An) decreases with increasing pH. It hinders the An-to-Np approach and weakens the quenching effect. (ii) A less dense inner shell allows a deeper penetration hydrophobic An acceptors which come closer to the interface-localized Np. It promotes the quenching effect. At pH close to pK_A, the second effects wins and the efficiency of energy transfer grows. With a further increase in pH, the ionization increases and electrostatic forces become strong. The shell forming PMA chains stretch and the fraction of An located close to the core decreases drastically. This is witnessed by a pronounced decrease of the quenching effect. Nevertheless, even at pH ca. 10, the NRET quenching effect is not negligible.

Conclusion

The conformational behavior of shell-forming chains of PS-PMA micelles, modified by attachment of a strongly hydrophobic group at the free PMA end, differs from that of non-modified parent systems. The H group tries to avoid the aqueous environment and buries in the shell forcing PMA chains to collapse. The distribution of H groups in the shell is a result of an intricate enthalpy-to-entropy interplay. Increasing ionization of PMA (with increasing pH) generally promotes the chain stretching, but the NRET measurements indicate bimodal distribution of H distances from the core and a non-monotonous dependence of NRET efficiency on pH.

Acknowledgements: The authors would like to thank the Grant Agency of the Academy of Sciences of the Czech Republic (Grant IAA401110702), Grant Agency of Czech Republic (Grant 203/07/0659) and the Ministry of Education of the Czech Republic (Long term research plan MSM0021620857).

[1] M. Štěpánek, K. Procházka, *Langmuir* **1999**, *15*, 8800.
[2] C. Heitz, M. Rawiso, J. Francois, *Polymer* **1999**, *40*, 1637.
[3] V. N. Bliznyuk, H. E. Assender, G. A. D. Briggs, *Macromolecules* **2002**, *35*, 6613.
[4] T. Azzam, A. Eisenberg, *Angewandte Chemie – Internat. Ed.* **2006**, *45*, 7443.
[5] D. Wang, J. Yin, Z. Y. Zhu, Z. S. Ge, H. W. Liu, S. P. Armes, S. Y. Liu, *Macromolecules* **2006**, *39*, 7378.
[6] S. Förster, V. Abetz, A. H. E. Müller, *Advances in Polymer Science* **2004**, *166*, 173.
[7] D. V. Pergushov, E. V. Remizova, J. Felthusen, A. B. Zezin, A. H. E. Müller, V. A. Kabanov, *J. Phys. Chem. B* **2003**, *107*, 8093.
[8] R. K. O'Reilly, C. J. Hawker, K. L. Wooley, *Chem. Soc. Rev.* **2006**, *35*, 1068.
[9] Y. Mitsukami, A. Hashidzume, S. Yusa, Y. Morishima, A. B. Lowe, C. L. McCormick, *Polymer* **2006**, *47*, 4333.
[10] R. Savic, A. Eisenberg, D. Maysinger, *J. Drug Targeting* **2006**, *14*, 343.
[11] A. Harada, K. Kataoka, *Progress Polym.Sci.* **2006**, *31*, 949.
[12] M. Štěpánek, K. Podhájecká, K. Procházka, Y. Teng, S. E. Webber, *Langmuir* **1999**, *15*, 4185.
[13] M. Pacovská, K. Procházka, Z. Tuzar, P. Munk, *Polymer* **1993**, *34*, 4585.
[14] J. Pleštil, J. Kříž, Z. Tuzar, K. Procházka, Y. B. Melnichenko, G. D. Wignall, P. Munk, S. E. Webber, *Macromol. Chem. Phys.* **2001**, *202*, 553.
[15] P. Matějíček, K. Podhájecká, J. Humpolíčková, F. Uhlík, K. Jelínek, Z. Limpouchová, K. Procházka, M. Špírková, *Macromolecules* **2004**, *37*, 10141.
[16] J. Humpolíčková, M. Štěpánek, K. Procházka, M. Hof, *J. Phys. Chem. A* **2005**, *109*, 10803.
[17] F. Uhlík, Z. Limpouchová, K. Jelínek, K. Procházka, *J. Chem. Phys.* **2004**, *121*, 2367.
[18] P. Matějíček, F. Uhlík, Z. Limpouchová, K. Procházka, Z. Tuzar, S. E. Webber, *Macromolecules* **2002**, *35*, 9487.

[19] K. Jelínek, Z. Limpouchová, F. Uhlík, K. Procházka, *Macromolecules* **2007**, *40*, 7656.
[20] F. Uhlík, K. Jelínek, Z. Limpouchová, K. Procházka, *Macromolecules* in press.
[21] M. Štěpánek, K. Krijtová, K. Procházka, *Acta Polymerica* **1998**, *49*, 96.
[22] J. Humpolíčková, K. Procházka, M. Hof, Z. Tuzar, M. Špírková, *Langmuir* **2003**, *19*, 4111.
[23] M. A. Karymov, K. Procházka, J. M. Mendelhall, S. E. Webber, *Langmuir* **1996**, *12*, 4748.
[24] F. Uhlík, Z. Limpouchová, K. Jelínek, K. Procházka, *J. Chem. Phys.* **2003**, *118*, 11258.
[25] U. Strauss, G. Vesnauer, *J. Phys. Chem.* **1975**, *79*, 1558.
[26] Y. Wang, H. Morawetz, *Macromolecules* **1986**, *19*, 1925.
[27] K. P. Ghiggino, K. L. Tan, in: *Polymer Photophysics*, D. Phillips, Ed., *Chapman and Hall*, London **1985**.
[28] M. Štěpánek, K. Procházka, W. Brown, *Langmuir* **2000**, *16*, 2502.
[29] S. Förster, N. Hermsdorf, C. Bottcher, P. Lindner, *Macromolecules* **2002**, *35*, 4096.
[30] S. Förster, V. Abetz, A. H. E. Müller, *Adv. Polym. Sci.* **2004**, *166*, 173.

